Available online at www.sciencedirect.com

ScienceDirect

IFAC PapersOnLine 56-1 (2023) 79–84

Noise Sensitivity Reduction in Low-power Multi High Gain Observers Using Low-pass Filters

S. Mousavi * **M. Guay** **

* *Queen's University, 99 University Ave, Kingston, ON K7L 3N6, Canada (e-mail: s.mousavi@queensu.ca).*

** *Queen's University, 99 University Ave, Kingston, ON K7L 3N6, Canada (e-mail: guaym@queensu.ca).*

Abstract: Low-power multi high gain observers (LP MHGO) are proven to be effective in reducing the peaking of state estimation of nonlinear systems to an arbitrarily small magnitude. Moreover, they reduce the sensitivity of estimates to measurement noise. They also relax the numerical implementation problem of high gain observers by using gains powered up to the order of 2 instead of n. In this paper, we aim to further reduce the noise sensitivity of these observers by employing low-pass filters in the observer dynamics. The main results establish the convergence of the estimation error to zero with an arbitrarily small decay rate in the absence of noise, as well as an input to state stability feature when the noise is present. We also demonstrate in the linear case that the proposed observer improves the upper bound on the estimates. Simulation results compare the performance of the proposed observer with similar works and show the effectiveness of the proposed method.

Keywords: Observers for nonlinear systems; Nonlinear output feedback; Nonlinear systems

1. INTRODUCTION

High gain observers (HGO) have received great attention in the control literature due to their simplicity and robustness, Khalil and Praly (2014). Their main feature is their ability to assign an arbitrarily small decay rate of the estimation errors that can be chosen using a design parameter (in this paper, called ϵ). More importantly, they provide a nonlinear separation principle when they are used to implement stabilizing state feedback controllers, Atassi and Khalil (1999). Unfortunately, they are susceptible to two major problems that have been the subject of many works in the past three decades:

- **Peaking phenomenon:** As ϵ is decreased to provide faster convergence of the estimates, a larger impulse overshoot develops in the transient response. The overshoot, with growth of order ϵ^{1-n} can destabilize the closed loop system. A trade-off between the fast convergence of estimates and small peaking must be considered when choosing ϵ, Sussmann and Kokotovic (1991).
- **Noise sensitivity:** Although the estimates remain stable in the presence of measurement noise, the noise can lead to large steady-state oscillations of order ϵ^{-n} and yield a larger upper bound on the estimation errors, Vasiljevic and Khalil (2006).

Time varying gains proposed in Ibrir and Diop (1999), Ibrir (2001), and Ibrir (2004) are shown to be an effective method for peaking attenuation of HGOs, Chitour (2002). These observers use dynamic gains that start small and grow over time to reach high gains. An alternative switched gain method is proposed in Ahrens and Khalil (2009) to deal with the noise sensitivity. The strategy is to use high gains initially and gradually reduce them to mitigate the possibility of large steady-sate oscillations.

An adaptive approach, called Multi high gain observers (MHGO), is also suggested in Shakarami et al. (2018) and Shakarami et al. (2020) for peaking elimination. A MHGO uses multiple HGOs simultaneously, and aggregates all the estimates obtained from each observer using some coefficients (some of which are equal to 1). It is shown that this method is quite effective in terms of peaking reduction since the upper bound on the transient response of the error is proportional to a design parameter that can be chosen arbitrarily.

An in-depth analysis of noise sensitivity is provided in Astolfi et al. (2016) to capture the low-pass filtering characteristics of HGOs. It is shown that the steady state bound on the estimate errors is proportional to the inverse of noise frequency, ε. This means that a higher frequency noise can effectively reduce the upper bound on the estimates. The upper bound depends on the relative degree between the estimation error and the output measurement. The lower sensitivity to noise as the relative degree increases is indeed the main reason for the implementation of low-power observers as discussed in Astolfi and Marconi (2015) and Astolfi et al. (2018). An alternative approach is utilizing low pass filters to improve the low-pass filtering feature of a HGO. This approach has been the focus of some recent works (see for example Khalil and Priess (2016),Tréangle et al. (2019) and Astolfi et al. (2021). It is demonstrated in Astolfi et al. (2021) that

10.1016/j.ifacol.2023.02.014

the new bound for the proposed observer is multiplied by higher powers of ε.

A low-power multi high gain observer is also proposed in Mousavi and Guay (2021) by combining low-power observer and MHGO designs. It is proved that all the nice features including arbitrarily small peaking and reduced noise sensitivity remain valid for the new design. In this work, we apply the approach proposed in Astolfi et al. (2021) to low-power MHGO to improve the performance of MHGO in the presence of noise. We propose the application of low-pass filters in low-power observers to reduce the ultimate estimate error, and employ this observer in a MHGO design to eliminate the peaking.

The paper is organized as follows: Section 2 includes the problem formulation and some preliminaries about high gain observers. The proposed observer design is given in section 3, followed by stability and noise sensitivity analysis in section 4. Section 5 uses a numerical example to compare the new design to some other observers. Finally, section 6 concludes the main results of the paper.

2. PRELIMINARIES AND PROBLEM FORMULATION

In this paper, we consider nonlinear SISO systems in their canonical observable form, Gauthier and Kupka (2001):

$$\begin{aligned}\dot{x}_i &= x_{i+1}, \quad i = 1, \dots, n-1,\\ \dot{x}_n &= f(x, u),\\ y &= x_1 + v\end{aligned} \tag{1}$$

where $x = [x_1, \dots, x_n]^T \in R^n$ is the vector of state variables, $u \in \mathcal{U} \subseteq R$ and $y \in R$ are the system's input and output variables, respectively. One can compactly write system (1) as

$$\begin{aligned}\dot{x} &= A_n x + B_n f(x, u)\\ y &= C_n x + v\end{aligned}$$

where the matrices $A_n \in R^{n\times n}$, $B_n \in R^{n\times 1}$ and $C_n \in R^{1\times n}$ are given as follows

$$A_n = \begin{bmatrix} 0_{(n-1)\times 1} & I_{n-1} \\ 0 & 0_{1\times(n-1)} \end{bmatrix}$$

$$B_n = \begin{bmatrix} 0_{1\times(n-1)} & 1 \end{bmatrix}^T, C_n = \begin{bmatrix} 1 & 0_{1\times(n-1)} \end{bmatrix}$$

where I_{n-1} is the $n-1 \times n-1$ identity matrix. We assume that $f(x, u)$, with $f(0, 0) = 0$, is locally Lipschitz vector function in x for all $x \in \mathcal{X} \subseteq R^n$, where $\mathcal{X}$ is a bounded set. We suppose that there exist convex sets $\mathcal{U}, \mathcal{X}, \mathcal{X}_0$ such that for any initial conditions satisfying $x(0) \in \mathcal{X}_0 \subset \mathcal{X} \subset R^n$ and any $u \in \mathcal{U}$, the solution of system (1) remains in $\mathcal{X}$ for all $t \geq 0$. As in Astolfi et al. (2016), we model the measurement noise as a finite sum of sinusoids, namely

$$v(t) = \sum_{i=1}^{n_v} v_i \sin(\frac{\omega_i}{\varepsilon} t + \phi_i). \tag{2}$$

where ϕ_i and v_i denote the phase and amplitude of each component, and where ω_i characterizes the basic frequency that is made to increase as $\varepsilon \to 0$. It is also assumed that $v(t)$ is bounded, i.e., there exists a $\mu > 0$ such that $\|v(t)\| \leq \mu$ for all $t \geq 0$. A conventional high gain observer for system (1) is designed as

$$\dot{\hat{\xi}} = A_n\hat{\xi} + B_n f_s\left(\hat{\xi}, u\right) + \Gamma_1^{-1} K_n \tilde{\xi} \tag{3}$$

where $\tilde{\xi} = \left(y - C_n\hat{\xi}\right)$, $\epsilon \in (0, 1]$,

$$\Gamma_1(\varepsilon) = \mathrm{diag}(\epsilon, \epsilon^2, \epsilon^2, \dots, \epsilon^n),$$

and the vector $K_n = [k_1, k_2, \dots, k_n]^T$ is tuned such that the matrix $A_n - K_n C_n$ is Hurwitz. The globally bounded and locally Lipschitz function $f_s(.)$ is a saturated version of $f(.)$ that agrees with $f(.)$ on $\mathcal{X} \times \mathcal{U}$ and satisfies

$$\|f(x, u) - f_s(\hat{x}, u)\| \leq \bar{f}\|x - \hat{x}\| \tag{4}$$

for a positive constant $\bar{f}$. If $f(.)$ is globally Lipschitz, then we can allow f_s to be equal to f. It is shown that for a small enough ϵ, the following bound is obtained for the estimation errors, Khalil and Praly (2014),

$$\|x_i(t) - \hat{\xi}_i(t)\| \leq \rho_1\epsilon^{1-i} exp(-\frac{\rho_2}{\epsilon}t)|x(0) - \hat{\xi}(0)| + \rho_3\epsilon^{1-i}\mu \tag{5}$$

for some $\rho_1, \rho_2, \rho_3 > 0$ that are independent of ϵ, and all initial conditions in $\mathcal{X}_0$. The bound (5) expresses the convergence of the estimation errors in the absence of noise. It also highlights the input to state stability property of an HGO in the presence of noise. It also shows the trade off between the fast convergence rate, which depends on ϵ, the peaking and the sensitivity to noise that increase as smaller values are chosen for ϵ. The characterization of sensitivity of HGO to the high-frequency noise is performed in Astolfi et al. (2016) where the following bound is obtained for the asymptotic behavior of the estimates

$$\lim_{t\to\infty} \sup |x_i(t) - \hat{\xi}_i(t)| \leq \frac{\hat{\rho}\varepsilon}{\epsilon^i}\mu. \tag{6}$$

The above bound captures the low-pass filtering feature of a HGO. It shows that the upper bounds on the estimates decrease as the frequencies of the noise increase. One can see that (6) is of order one in ε which is the relative degree between y and all the estimates in the HGO. A modified version of a HGO is proposed in Astolfi et al. (2021) where this relative degree is increased to $r+1$ using a cascade of low-pass filters. In this design, the filters are given by

$$\begin{aligned}\dot{\eta}_1 &= -\frac{1}{\zeta\epsilon}(\eta_1 - (y - C_n\hat{\xi})),\\ \dot{\eta}_i &= -\frac{1}{\zeta\epsilon}(\eta_i - \eta_{i-1}), \qquad i = 2, \dots, r,\\ \tilde{\xi} &= \eta_r\end{aligned} \tag{7}$$

Compactly written as $\dot{\eta} = -\frac{1}{\zeta\epsilon}(I_r - A_r^T)\eta + \frac{1}{\zeta\epsilon}C_r^T(y - C_n\hat{\xi})$, $\tilde{\xi} = B_r^T z$ where ζ is some positive parameter that must be assigned. It is proved that for small enough ζ, ϵ and for $\eta(0) = 0$, the observer (3), (7) yields the bound (5). Moreover, using the ideas from Astolfi et al. (2016), it is shown that the high-gain observer (3), (7) improves the bound (6) as

$$\lim_{t\to\infty} \sup |x_i(t) - \hat{\xi}_i(t)| \leq (\frac{\varepsilon}{\epsilon\zeta})^r \frac{\hat{\rho}\varepsilon}{\epsilon^i}\mu \tag{8}$$

One can see from (8) that the new bound depends on higher degrees of ε. As a result, the steady-state bound on the estimation error is smaller than a HGO when a high-frequency noise affects the output.

3. THE PROPOSED OBSERVER

The dynamics of the observer is presented in this section. Similar to Astolfi et al. (2021), we are interested in augmenting the relative degree between the estimates and the measured output y. We employ the same structure suggested in Mousavi and Guay (2021) that consists of two interconnected systems. While multiple low-power observers are employed in the first layer to estimate the states at the same time, all the information is used in the second layer to generate the final estimate. The existence of some unknown coefficients is proven for which the overall estimation reaches the true state variables. Hence, the second layer estimates these constants using a recursive least-squares (RLS) algorithm. The structure of each individual low-power observer is given as

$$\begin{aligned}
\dot{\hat{x}}_{i(j)} &= z_{i(j)} + \frac{a_i}{\epsilon}\tilde{e}_{i(j)}, && i = 1, \ldots, n-2\\
\dot{\hat{x}}_{n-1(j)} &= \hat{x}_{n(j)} + \frac{a_{n-1}}{\epsilon}\tilde{e}_{n-1(j)}\\
\dot{\hat{x}}_{n(j)} &= f_s\left(\sum_{j=1}^{n+1}\hat{\theta}_j\hat{x}_{(j)}, u\right) + \frac{b_{n-1}}{\epsilon^2}\tilde{e}_{n-1(j)}\\
\dot{z}_{i(j)} &= z_{i+1(j)} + \frac{b_i}{\epsilon^2}\tilde{e}_{i(j)}, && i = 1, \ldots, n-3\\
\dot{z}_{n-2(j)} &= \hat{x}_n(j) + \frac{b_{n-2}}{\epsilon^2}\tilde{e}_{n-2(j)}
\end{aligned} \tag{9}$$

where $\epsilon \in (0, 1]$ is the design parameter that should be taken small enough to ensure the stability of the observer, and it is powered up to 2 (instead of n), $\hat{\theta}$ is the estimate of the unknown parameters, $\hat{x}_{(j)} = \left[\hat{x}_{1(j)}, \ldots, \hat{x}_{n(j)}\right]^T \in R^n$ denotes the estimate of state variables from the j^{th} observer for $j = 1, \ldots, n+1$, and $z_{(j)} = \left[z_{1(j)}, \ldots, z_{n-2(j)}\right]^T \in R^{n-2}$ are the additional estimates of $[x_2, \ldots, x_{n-1}]$. Also, $\underline{a} = col\,(a_1, \ldots, a_{n-1}) \in R^{n-1}$ and $\underline{b} = col\,(b_1, \ldots, b_{n-1}) \in R^{n-1}$ are the observer gains. In Mousavi and Guay (2021), the injection terms $\tilde{e}_{i(j)}$ are given by $\tilde{e}_{1(j)} = y - \hat{x}_{1(j)}, \tilde{e}_{i(j)} = z_{i-1(j)} - \hat{x}_{i(j)}$. In this design, we pass $\tilde{e}_{1(j)}$ through the filters (7) to reduce the vulnerability of the observer to noise. So, we have

$$\begin{aligned}
\dot{\eta}_{1(j)} &= -\frac{1}{\zeta\epsilon}(\eta_{1(j)} - (y - C_n\hat{x}_{(j)})),\\
\dot{\eta}_{i(j)} &= -\frac{1}{\zeta\epsilon}(\eta_{i(j)} - \eta_{i-1(j)}), && i = 2, \ldots, r,\\
\tilde{e}_{1(j)} &= \eta_{r(j)}\\
\tilde{e}_{i(j)} &= z_{i-1(j)} - \hat{x}_{i(j)}, && i = 2, \ldots, n-1
\end{aligned} \tag{10}$$

for $j = 1, \ldots, n+1$. We define $\tilde{y}\,(t) = y - C\hat{X}_{(n+1)}(t)$ where

$$\begin{aligned}
X &= [x_1, x_2, x_2, \ldots, x_{n-1}, x_{n-1}, x_n]^T,\\
\hat{X} &= [\hat{x}_1, z_1, \hat{x}_2, z_2, \ldots, z_{n-2}, \hat{x}_{n-1}, \hat{x}_n]^T.
\end{aligned}$$

And $C = [C_n \; 0_{n-2}]$. Now, let us establish the parameter update strategy as follows:

$$\begin{aligned}
\dot{\hat{\underline{\theta}}} &= -PE^TC^T\left(\tilde{y} + CE\hat{\underline{\theta}}\right), && \hat{\underline{\theta}}\,(0) = \hat{\underline{\theta}}_0\\
\dot{P} &= -PE^TC^TCEP, && P\,(0) = \gamma I
\end{aligned} \tag{11}$$

where $\hat{\underline{\theta}} \in \mathbb{R}^{n\times 1}$ denotes the vector of $\hat{\theta}_j$s for $j = 1, \ldots, n$, $P \in R^{n\times n}$ is a positive definite matrix. The parameter $\gamma \in R$ is a positive constant taken large enough to guarantee that the parameter estimation error and the peaking of the state estimates remain small, as discussed in Mousavi and Guay (2021). Matrix $E \in R^{(2n-2)\times n}$ is a matrix whose jth column is given by $\hat{X}_{(n+1)} - \hat{X}_{(j)}$ where $\hat{X}_{(j)}$ represents the vector $\hat{X}$ obtained from the jth observer, for $j = 1, \ldots, n+1$. The variables θ_j are supposed to be subject to the constraint $\sum_{i=1}^{n+1}\theta_j = 1$. So, we enforce $\hat{\theta}_{n+1} = 1 - \sum_{i=1}^{n}\hat{\theta}_j$. Finally, the overall observer estimation is calculated as

$$\hat{X}_o = \sum_{j=1}^{n+1}\hat{\theta}_j\hat{X}_{(j)} \tag{12}$$

where $\hat{X}_o\,(t) = [\hat{x}_{o1}, z_{o1}, \hat{x}_{o2}, z_{o2}, \ldots, \hat{x}_{o_n}]^T \in R^{2n-2}$. The parameters $\underline{a}, \underline{b}$ in (9) are chosen such that the block-tridiagonal matrix $M_\epsilon \in R^{(2n-2)\times(2n-2)}$, given below, is Hurwitz, Astolfi and Marconi (2015)

$$M_\epsilon = \begin{bmatrix}
J_1 & H & 0 & \cdots & \cdots & 0\\
Q_2 & J_2 & H & \ddots & & \vdots\\
0 & \ddots & \ddots & \ddots & \ddots & \vdots\\
\vdots & \ddots & \ddots & \ddots & \ddots & 0\\
\vdots & & \ddots & Q_{n-2} & J_{n-2} & H\\
0 & \cdots & \cdots & 0 & Q_{n-1} & J_{n-1}
\end{bmatrix}. \tag{13}$$

The matrices $H \in R^{2\times 2}$ and $J_i, Q_i \in R^{2\times 2}, i = 1, \ldots, n-1$ are defined as:

$$H = \begin{bmatrix} 0 & 0\\ 0 & 1\end{bmatrix}, J_i = \begin{bmatrix} -\frac{a_i}{\epsilon} & 1\\ -\frac{b_i}{\epsilon^2} & 0\end{bmatrix}, Q_i = \begin{bmatrix} 0 & \frac{a_i}{\epsilon}\\ 0 & \frac{b_i}{\epsilon^2}\end{bmatrix}$$

where $i = 1, \ldots, n-1$. We denote the matrix M to be equal to M_ϵ for $\epsilon = 1$. It is clear that the Hurwitz property of M and M_ϵ are equivalent. At the end of this section, we present a lemma taken from Astolfi et al. (2021) that will be useful in proving the main results presented in section 4.

Lemma 1. Let K_n be such that $A_n - \Gamma_1^{-1}K_nC_n$ is Hurwitz. Then, for each $r \in N_{>0}$, there exists $\zeta^* > 0$ such that for any $\zeta \in (0, \zeta^*)$, the matrix $F(\zeta)$ given below is Hurwitz.

$$F(\zeta) := \begin{bmatrix} A_n & -\Gamma_1^{-1}K_nB_r^T\\ \frac{1}{\zeta}C_r^TC_n & -\frac{1}{\zeta}(I_r - A_r^T)\end{bmatrix} \tag{14}$$

Proof: See Astolfi et al. (2021). ∎

The stability and convergence of the observer, as well as improved performance in terms of sensitivity to noise, is proven in the following section.

4. PERFORMANCE ANALYSIS

We investigate the performance of the suggested observer in terms of convergence and steady state bounds in the presence of high-frequency noise. We first show that the proposed observer (9)-(12) holds the same features of arbitrary small convergence rate and the stability to noise. These results are highlighted in the following theorem.

Theorem 1. Let the trajectories of (1) be such that $x \in \mathcal{X}$ for all $u \in \mathcal{U}$, and let the noise be generated by (2). For the observer (9)-(12), fix the order of filters r, and tune $\underline{a}, \underline{b}$ in (9) such that M is Hurwitz. Let the initial conditions of all the filters to be 0, and choose $z_{i(j)}\,(0) = \hat{x}_{i+1(j)}(0)$ for $i = 1, \ldots, n-2, j = 1, \ldots, n+1$, and select $\hat{x}_{i(j)}(0)$s such that the matrix $E(0)$ has full column rank. Then there exists a ζ^* such that if one chooses $\zeta \in (0, \zeta^*)$, there exists an $\epsilon^* > 0$ and some positive constants ρ_1, ρ_2 and ρ_3 such that for all $0 < \epsilon \leq \epsilon^*$, the state estimates obtained from (12) satisfy

$$\|x_i(t) - \hat{x}_{oi}(t)\| \leq \rho_1 \epsilon^{1-i} exp(-\frac{\rho_2}{\epsilon} t)|x(0) - \hat{x}_o(0)| + \rho_3 \epsilon^{1-i} \mu \tag{15}$$

Proof: Let us define $e = X - \hat{X}_o$, $e_{(j)} = X - \hat{X}_{(j)}$ and use (12) to write:

$$e = \sum_{j=1}^{n+1} \hat{\theta}_j e_{(j)} = e_{(n+1)} + E\hat{\tilde{\theta}} \tag{16}$$

Employing (9) and (10), one can get the error dynamics for each individual observer as

$$\begin{aligned}\dot{e}_{(j)} &= \tilde{M}_\epsilon e_{(j)} - \tilde{K}_\epsilon B_r^T \eta_{(j)} + B(f(x,u) - f_s(\hat{x}_o, u)) \\ \dot{\eta}_{(j)} &= -\frac{1}{\zeta\epsilon}(I_r - A_r^T)\eta_{(j)} + \frac{1}{\zeta\epsilon} C_r^T (Ce_{(j)} + v)\end{aligned} \tag{17}$$

where $B = [0_{(1)\times(n-2)} \quad B_n^T]^T$, $\tilde{M}_\epsilon$ is M_ϵ with changing only J_1 to $\begin{bmatrix}0 & 1\\ 0 & 0\end{bmatrix}$ (similarly, $\tilde{M}$ is equal to M for the same J_1), and $\tilde{K}_\epsilon = [\frac{a_1}{\epsilon}, \frac{b_1}{\epsilon^2}, \quad 0_{(1)\times(2n-4)}]^T$ (Also, define $\tilde{K}$ equal to $\tilde{K}_\epsilon$ for $\epsilon = 1$). Now define $\Gamma(\varepsilon) = \text{diag}\left(1, \epsilon, \epsilon, \epsilon^2, \epsilon^2, \ldots, \epsilon^{n-2}, \epsilon^{n-2}, \epsilon^{n-1}\right)$, and consider the coordinate change $\psi_{(j)} := [\begin{smallmatrix}\Gamma e_{(j)}\\ \eta_{(j)}\end{smallmatrix}]$, the time rescaling $t \to \tau(t) := \frac{t}{\epsilon}$, and recall the properties $C\Gamma^{-1} = C\Gamma = C, \Gamma B = \epsilon^{n-1}B, \Gamma\tilde{K}_\epsilon = \frac{1}{\epsilon}\tilde{K}$ and $\Gamma\tilde{M}_\epsilon\Gamma^{-1} = \frac{1}{\epsilon}\tilde{M}$ to write

$$\frac{d\psi_{(j)}}{d\tau} = \tilde{F}\psi_{(j)} + \epsilon\mathcal{H}\Delta(\hat{x}_o, x, u) + \frac{1}{\zeta}Gv. \tag{18}$$

where $\tilde{F}$, $\mathcal{H}$ are given by:

$$\begin{aligned}\tilde{F} &:= [\begin{smallmatrix}\tilde{M} & -\tilde{K}B_r^T \\ \frac{1}{\zeta}C_r^T C & -\frac{1}{\zeta}(I_r - A_r^T)\end{smallmatrix}], \\ \mathcal{H} &:= (B^T, 0_{1\times r})^T, G := (0_{1\times(2n-2)}, C_r)^T\end{aligned} \tag{19}$$

$$\Delta(\hat{x}_o, x, u) := \epsilon^{n-1}[f(x,u) - f_s(\hat{x}_o, u)] \tag{20}$$

Now let us use the results of lemma 1 to show the matrix $\tilde{F}$ in (18) is Hurwitz. Comparing (19) and (14), one can see that $\tilde{F}$ is equal to F by replacing $A_n, C_n, \Gamma_1^{-1}K_n$ with $\tilde{M}, C, \tilde{K}$, respectively. So, to show that the matrix $\tilde{F}$ is Hurwitz, it is sufficient to check that $\tilde{M} - \tilde{K}C$ (equivalent to $A_n - \Gamma_1^{-1}K_nC_n$ in (14)) is Hurwitz. Since $\tilde{M} - \tilde{K}C = M$ is Hurwitz by selection of $\underline{a}, \underline{b}$ (see Lemma 1 in Astolfi and Marconi (2015)), then there exists a ζ^* such that if one chooses $\zeta \in (0, \zeta^*)$, $\tilde{F}$ is Hurwitz. Hence, there exists a symmetric positive definite matrix $\tilde{P} \in R^{(2n-2+r)\times(2n-2+r)}$ such that

$$\tilde{P}\tilde{F} + \tilde{F}^T\tilde{P} = -I_{(2n-2+r)}. \tag{21}$$

By defining the matrix $E_\psi \in R^{(2n-2+r)\times n}$ whose jth column is equal to $\psi_{(j)} - \psi_{(n+1)}$, we can write (16) as

$$\psi = \psi_{(n+1)} + E_\psi\hat{\tilde{\theta}} \tag{22}$$

Where $\psi = [\begin{smallmatrix}\Gamma e\\ \eta\end{smallmatrix}] = \sum_{j=1}^{n+1}\psi_{(j)}$. On the other hand, the dynamics of E_ψ can be easily obtained using (18) as

$$\frac{dE_\psi}{d\tau} = \tilde{F}E_\psi. \tag{23}$$

Taking the derivative of (22) with respect to τ, and using (11), (18), (23) and $\tau = \frac{t}{\epsilon}$, yields:

$$\begin{aligned}\frac{d\psi}{d\tau} =& \tilde{F}\psi_{(n+1)} + \epsilon\mathcal{H}\Delta(\hat{x}_o, x, u) + \frac{1}{\zeta}Gv \\ &+ \tilde{F}E_\psi\hat{\tilde{\theta}} - \epsilon E_\psi PE^TC^T(Ce + v).\end{aligned} \tag{24}$$

We define $\tilde{C} = (C, 0_{1\times r})$ and use $CE = \tilde{C}E_\psi, Ce = \tilde{C}\psi$, and (22) to write (24) as

$$\frac{d\psi}{d\tau} = \tilde{F}\psi + \epsilon\mathcal{H}\Delta(\hat{x}_o, x, u) + \frac{1}{\zeta}Gv - \epsilon E_\psi PE_\psi^T\tilde{C}^T(\tilde{C}\psi + v) \tag{25}$$

One can pose the Lyapunov candidate function $V(\psi) = \psi^T\tilde{P}\psi$ subject to (21), and use (25) to obtain

$$\begin{aligned}\frac{dV(\psi)}{d\tau} =& -\psi^T\psi - 2\epsilon\psi^T\tilde{P}E_\psi PE_\psi^T\tilde{C}^T\tilde{C}\psi \\ &+ 2\epsilon\psi^T\tilde{P}H\Delta(\hat{x}_o, x, u) \\ &- 2\epsilon\psi^T\tilde{P}E_\psi PE_\psi^T\tilde{C}^Tv + \frac{2}{\zeta}\psi^T\tilde{P}Gv\end{aligned}$$

Let us denote the smallest and the lagest eigenvalues of $\tilde{P}$ in (21) as $\underline{p}$ and $\bar{p}$, respectively. Furthermore, from (11) we have $\|P\| \leq \gamma$, and from (23), and the fact that $\tilde{F}$ is Hurwitz, we get $\|E_\psi\| \leq \hat{c}_1\|E_\psi(0)\|$ where $\hat{c}_1$ is some positive constant. Also, considering (20) and the definition of ψ we have $|\Delta(\hat{x}_o, x, u)| \leq \bar{f}\|\psi\|$. Using these bounds, and the following Young's inequality

$$\begin{aligned}&\|\psi^T(-2\epsilon\tilde{P}E_\psi PE_\psi^T\tilde{C}^T + \frac{2}{\zeta}\tilde{P}G)v\| \leq \\ &\frac{1}{2}\|\psi\|^2 + \frac{1}{2}\|(-2\epsilon\tilde{P}E_\psi PE_\psi^T\tilde{C}^T + \frac{2}{\zeta}\tilde{P}G)v\|^2 \leq \\ &\frac{1}{2}\|\psi\|^2 + 2\|v\|^2(\epsilon\bar{p}\hat{c}_1^2\|E_\psi(0)\|^2\gamma + \frac{\bar{p}}{\zeta})^2\end{aligned}$$

yields $\frac{dV(\psi)}{d\tau} \leq -\frac{1}{2}\|\psi\|^2(1 - 4\epsilon\bar{p}c_1) + 2(c_2\epsilon + c_3)^2\|v\|^2$, where $c_1 = \hat{c}_1^2\|E_\psi(0)\|^2\gamma + \bar{f}, c_2 = \bar{p}\hat{c}_1^2\|E_\psi(0)\|^2\gamma, c_3 = \frac{\bar{p}}{\zeta}$. We can now choose any $\epsilon^* < \min\{\frac{1}{4\bar{p}c_1}, 1\}$ such that there exists $\rho_2 > 0, c_4 > 0$ satisfying, for any $\epsilon \in (0, \epsilon^*)$, the inequalities $1 - 4\epsilon\bar{p}c_1 \geq 4\rho_2\bar{p}$ and $2(c_2\epsilon + c_3)^2 \leq c_4$. Then we get $\frac{dV(\psi(\tau))}{d\tau} \leq -2\rho_2V((\psi(\tau)) + c_4\|v(\tau)\|^2$. By using the comparison principle, we obtain

$$\begin{aligned}V(\psi(\tau)) \leq& \exp(-2\rho_2\tau)V(\psi(0)) \\ &+ \int_0^\tau \exp(-2\rho_2(\tau - s))c_4|v(s)^2|ds \\ \leq& \exp(-2\rho_2\tau)V(\psi(0)) + c_5\mu^2\end{aligned} \tag{26}$$

where $c_5 = \frac{c_4}{2\rho_2}$. The inequality (15) then follows by using $\underline{p}\|\psi\|^2 \leq V \leq \bar{p}\|\psi\|^2, \|\psi\|^2 \leq \|e\|^2 + \|\eta\|^2$, $\eta(0) = 0$, $\|x_i - \hat{x}_{oi}\| \leq \epsilon^{1-i}\|\psi\|$, $\tau = \frac{t}{\epsilon}$ with $\rho_1 = \sqrt{\frac{\bar{p}}{\underline{p}}}, \rho_3 = \sqrt{\frac{c_5}{\underline{p}}}$. ■

Remark 1. One can conclude from the proof of theorem 1 that the non-restrictive assumptions $z_{i(j)}(0) = \hat{x}_{i+1(j)}(0)$ and matrix $E(0)$ having full column rank, are not necessary to obtain the bound (15), but they are required for the peaking reduction feature of the proposed structure as discussed in Shakarami et al. (2020).

We can verify from (15) that the estimation error obtained from the proposed observer converges to zero with an arbitrarily fast convergence rate. We can also conclude that the observer is ISS with respect to noise. The next theorem characterizes the behaviour of the steady-state estimation error following the ideas presented in Astolfi et al. (2016, 2018).

Theorem 2. Consider system (1) where $x \in \mathcal{X}$ and $u \in \mathcal{U}$, and the observer (9)-(12), and define $m = \lceil \frac{n+1}{2} \rceil$. Choose any stabilizing selection of $\underline{a}, \underline{b}, \zeta, r$, and let the noise generated by (2). Then, there exists some $\varepsilon^*(\epsilon)$ and $\hat{\kappa} > 0$ such that for all positive $\varepsilon \leq \varepsilon^*(\epsilon)$ we have

$$\begin{aligned} &\lim_{t\to\infty} \sup |x_i(t) - \hat{x}_{oi}(t)| \leq \hat{\kappa}_i (\frac{\varepsilon}{\epsilon\zeta})^r \frac{\varepsilon^i}{\epsilon^{2i-1}} \mu \\ &for\ i = 1, \dots, m \\ &\lim_{t\to\infty} \sup |x_i(t) - \hat{x}_{oi}(t)| \leq \hat{\kappa}_i (\frac{\varepsilon}{\epsilon\zeta})^r \frac{\varepsilon^{n-i+2}}{\epsilon} \mu \\ &for\ i = m+1, \dots, n \end{aligned} \tag{27}$$

Proof: We consider the linear case where $f(x,u) = f_s(x,u) = \mathcal{F}x = \mathcal{F}LX$ where $\mathcal{F} \in R^{1\times n}$ is the vector of coefficients, with $|\mathcal{F}| \leq \bar{f}$, and $L \in R^{n\times(2n-2)} :=$ blkdiag$(C_2, \dots, C_2, I_2)$. The obtained bounds can also be extended to the nonlinear setting, as shown in Astolfi et al. (2016). We first model the noise (2) as the output of an autonomous system:

$$\begin{aligned} \varepsilon\dot{w} &= \mathcal{S}w,\ w \in R^{2n_v} \\ v &= \mathcal{P}w \end{aligned} \tag{28}$$

where the matrices $\mathcal{S} \in R^{2n_v\times 2n_v}, \mathcal{P} \in R^{1\times 2n_v}$ are given by $\mathcal{S} :=$ blkdiag$(\mathcal{S}_1, \dots, \mathcal{S}_{n_v})$, where $\mathcal{S}_i = \begin{bmatrix} 0 & \omega_i \\ -\omega_i & 0 \end{bmatrix}$, and $\mathcal{P} := [0\ 1\ 0\ 1\ \cdots\ 0\ 1]$. The system (28) may be thought of as a generator of n_v harmonics at the frequencies $\frac{\omega_i}{\varepsilon}$. Now consider $t = \tau\epsilon$ to re-write (25) as

$$\dot{\psi} = \frac{1}{\epsilon}\tilde{F}\psi + \epsilon^{n-1}\mathcal{H}\mathcal{F}L\tilde{\Gamma}\psi + \frac{1}{\zeta\epsilon}G\mathcal{P}w - D(t)(\tilde{C}\psi + \mathcal{P}w) \tag{29}$$

where $D(t) = E_\psi P E_\psi^T \tilde{C}^T$ is a time-varying term that goes to zero in time due to the dynamics (23), and $\tilde{\Gamma} = (\Gamma_{2n-2}^{-1}, 0_{(2n-2)\times(r)})$. We compactly write (29) as $\dot{\psi} = \Psi\psi + \Omega\mathcal{P}w - D(\tilde{C}\psi + \mathcal{P}w)$. To show the Hurwitzness of $\Psi = \frac{1}{\epsilon}\tilde{F} + \epsilon^{n-1}\mathcal{H}\mathcal{F}L\tilde{\Gamma}$, it is sufficient to see that, $\frac{1}{\epsilon}\tilde{F}$ is the dominant term in Ψ. Because $\tilde{F}, \mathcal{H}, \mathcal{F}$ and L do not depend on ϵ, and we have $|\epsilon^{n-1}\tilde{\Gamma}| \leq 1$. So, for sufficiently small ϵ, Ψ is Hurwitz. Let us now define $\tilde{\psi} = \psi - \Pi w$ and write:

$$\dot{\tilde{\psi}} = \Psi\tilde{\psi} + (\Psi\Pi + \Omega\mathcal{P} - \frac{1}{\varepsilon}\Pi\mathcal{S})w - D(t)\tilde{C}\tilde{\psi} - \hat{v} \tag{30}$$

where $\hat{v} = D(t)(\tilde{C}\Pi w + \mathcal{P}w)$. If we find Π such that $\Psi\Pi + \Omega\mathcal{P} - \frac{1}{\varepsilon}\Pi\mathcal{S} = 0$, then system (30) is an exponentially stable system and based on theorem 1, and assuming a solution Π for the Sylvester equation

$$\Pi\mathcal{S} = \varepsilon(\Psi\Pi + \Omega\mathcal{P}) \tag{31}$$

we can write $\tilde{\psi}_{ss} = \psi_{ss} - \Pi w = 0$ for the steady-state. Therefore, the steady-state behaviour of the error can be characterized by finding the solution to (31). Using the fact that the eigenvalues of $\mathcal{S}$ are on the imaginary axis and those of Ψ are all negative, the solution of (31) is unique, and it can be shown that

$$\Pi(\varepsilon) = \sum_{k=1}^{+\infty} \varepsilon^k \bar{\Pi}_k, \quad \bar{\Pi}_k = \Psi^{k-1}\Omega\mathcal{P}\mathcal{S}^{-k} \tag{32}$$

satisfies (31). By using $x - \hat{x}_o = L\tilde{\Gamma}\psi$ and denoting by π_i the ith row of the matrix $L\tilde{\Gamma}$, we get $x_i(t) - \hat{x}_{oi}(t) = \pi_i\psi$ for $i = 1, \dots, n$. Now, we can write

$$\lim_{t\to\infty} \sup |x_i(t) - \hat{x}_{oi}(t)| = \lim_{t\to\infty} \sup |\pi_i \Pi w(t)|. \tag{33}$$

Moreover, using the definition (19), one can check that for $k = 1, \dots, r$ we have $\pi\Psi^{k-1}\Omega = 0$. Now let $\hat{k}_i$s be some positive constants depending on $\underline{a}, \underline{b}, \mathcal{F}$. By letting $i = 1$, we get $|\pi_1\varepsilon^{r+1}\Psi^r\Omega| = \hat{k_1}\frac{\varepsilon^{r+1}}{\zeta^r\epsilon^{r+1}}$. Considering the fact that for a small ε, the dominant term in (32) is the smallest power of ε, we write

$$|\pi_1\Pi| = \pi_1\varepsilon^{r+1}\Psi^r\Omega|\mathcal{P}\mathcal{S}^{-k}| + \sum_{r+2}^{\infty}|\pi_1\bar{\Pi}_k| \quad \leq \hat{k_1}\frac{\varepsilon^{r+1}}{\zeta^r\epsilon^{r+1}}. \tag{34}$$

Besides, $\pi_i\varepsilon^{r+1}\Psi^r\Omega = 0$ for $i = 2, \dots, n$. Now we let $i = 2$ to get $|\pi_2\varepsilon^{r+2}\Psi^{r+1}\Omega| = \hat{k_2}\frac{\varepsilon^{r+2}}{\zeta^r\epsilon^{r+3}}$ and $|\pi_n\varepsilon^{r+2}\Psi^{r+1}\Omega| = \hat{k_n}\frac{\varepsilon^{r+2}}{\zeta^r\epsilon^{r+1}}$. The rest of the proof is then to follow the same steps for $i = 3, \dots, m$ and combining the bounds on $\pi_i\Pi$ with (33) to verify (27), for a small ε and the constants $\hat{\kappa}_i$s taken as independent of $\varepsilon, \epsilon, \zeta$. ■

Theorem 2 shows that, as a result of using filters (7), the steady-state bound of the estimation error is multiplied by the term $(\frac{\varepsilon}{\epsilon\zeta})^r$ compared to a single low-power observer Astolfi and Marconi (2015), which is similar to the results obtained in Astolfi et al. (2021) for a filtered HGO compared to a single HGO (compare (6) and (8)).

5. SIMULATION STUDY

We consider the Rössler (chaotic) oscillator, Chlouverakis and Sprott (2006), to compare the proposed method to some traditional observers. By performing a coordinate change, one can describe a Rössler oscillator by (1) with $n = 3$ and

$$\begin{aligned} f(x) = u &- \beta x_1 + (\alpha\beta - 1)x_2 + (\alpha - \beta)x_3 \\ &+ (x_2 - \alpha x_1)(x_1 - ax_2 + x_3) \end{aligned} \tag{35}$$

where we have $\alpha = 0.5, \beta = 3, u = -1$. This simulation example was also used in Astolfi et al. (2021). The output of system (35) is given by $y(t) = x_1(t) + v(t)$ where $v(t) = 0.6sin(\frac{1}{\varepsilon}t) + sin(\frac{\sqrt{3}}{\varepsilon}t)$ with $\varepsilon = 10^{-3}$. System (35) is chaotic for the given parameters and the initial conditions $x(0) = [2, -2, 1]^T$. We compare the estimate errors using a FLP MHGO, a HGO, a Low-power observer and a filtered HGO. For all the observers, we place the poles at -1, which means $K_n = [3, 3, 1]^T$ for the HGO (3) and the filtered HGO (3), (7), and $a1 = a2 = b1 = 2, b2 = 0.5$ for a low-power observer (9) and a FLP MHGO (9)-(12). Also, we let $\epsilon = 0.05, \zeta = 0.1, \gamma = 10^3, r = 2$ (where applicable) throughout the simulation study. The initial conditions of the FLP MHGO are $\hat{x}_{(1)}(0) = [-4, -4, -4]^T, \hat{x}_{(2)}(0) = [-4, 4, 4]^T, \hat{x}_{(3)}(0) = [4, -4, 4]^T, \hat{x}_{(4)}(0) = [4, 4, -4]^T$. Since $\hat{\theta}(0) = [0, 0, 0, 1]^T$, we let $\hat{x}(0) = \hat{x}_{(4)}(0)$ for all the other observers to provide a fair comparison. Figure 1 compares the observer performances in estimating x_3. The figure illustrates that the suggested observer in this paper shows a better performance in terms of transient response. It also shows the steady-state responses where the FLP MHGO yields smaller steady-state oscillations

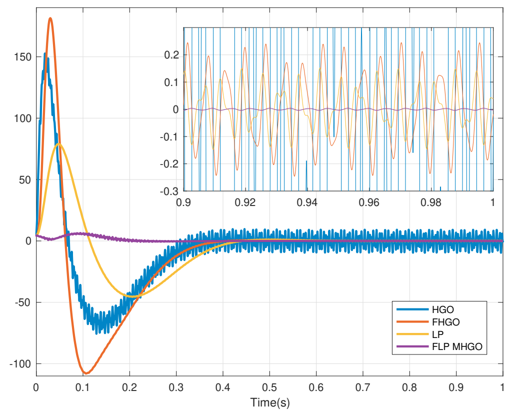

Fig. 1. State estimation error of x_3 in system (35) using a HGO, a filtered HGO (FHGO), a low-power observer (LP) and a filtered LP MHGO (FLP MHGO)

around zero. The steady-state values of all the estimation errors are given in Table 1 where we have defined $\|x_i(t) - \hat{x}_i(t)\|_s = \lim_{t\to\infty} \sup |x_i(t) - \hat{x}_i(t)|$. It is expected that the FHGO and the low-power perform better than a HGO, and that the FLP MHGO yields smaller steady state values compared to both LP and FHGO. The comparison of the LP and the FHGO shows that the low-power performs better than a FHGO for x_2 and x_3 and not for the x_1, which is also reasonable considering that the upper bounds on $x_1 - \hat{x}_1$ for the FHGO and the LP are proportional to $\frac{\varepsilon^3}{\zeta^2\epsilon^3} = 8 \times 10^{-4}$ and $\frac{\varepsilon}{\epsilon} = 2 \times 10^{-2}$, respectively.

Table 1. The steady state values of estimation errors using different observers

	HGO	FHGO	LP	FLP MHGO
$\|x_1 - \hat{x}_1\|_s$	0.0660	0.0018	0.0436	0.0012
$\|x_2 - \hat{x}_2\|_s$	1.3353	0.0358	0.0298	8.66×10^{-4}
$\|x_3 - \hat{x}_3\|_s$	9.1738	0.2386	0.1489	0.0043

6. CONCLUSION

This paper proposes a modification of low-power MHGOs that incorporates low-pass filters in the dynamics. The proposed observer is proven to be stable with an improved steady-state response in the presence of noise. The simulation results demonstrate the improvements of the proposed observer including peaking reduction and lower noise sensitivity compared to similar observers. The focus of the future work is to provide a nonlinear separation principle to use the observer in controller design.

REFERENCES

Ahrens, J.H. and Khalil, H.K. (2009). High-gain observers in the presence of measurement noise: A switched-gain approach. *Automatica*, 45(4), 936–943.

Astolfi, D. and Marconi, L. (2015). A high-gain nonlinear observer with limited gain power. *IEEE Transactions on Automatic Control*, 60(11), 3059–3064.

Astolfi, D., Marconi, L., Praly, L., and Teel, A. (2016). Sensitivity to high-frequency measurement noise of nonlinear high-gain observers. *IFAC-PapersOnLine*, 49(18), 862–866.

Astolfi, D., Marconi, L., Praly, L., and Teel, A.R. (2018). Low-power peaking-free high-gain observers. *Automatica*, 98, 169–179.

Astolfi, D., Zaccarian, L., and Jungers, M. (2021). On the use of low-pass filters in high-gain observers. *Systems & Control Letters*, 148, 104856.

Atassi, A.N. and Khalil, H.K. (1999). A separation principle for the stabilization of a class of nonlinear systems. *IEEE Transactions on Automatic Control*, 44(9), 1672–1687.

Chitour, Y. (2002). Time-varying high-gain observers for numerical differentiation. *IEEE Transactions on Automatic Control*, 47(9), 1565–1569.

Chlouverakis, K.E. and Sprott, J. (2006). Chaotic hyperjerk systems. *Chaos, Solitons & Fractals*, 28(3), 739–746.

Gauthier, J.P. and Kupka, I. (2001). *Deterministic observation theory and applications*. Cambridge university press.

Ibrir, S. (2001). New differentiators for control and observation applications. In *Proceedings of the 2001 American Control Conference.(Cat. No. 01CH37148)*, volume 3, 2522–2527. IEEE.

Ibrir, S. (2004). Linear time-derivative trackers. *Automatica*, 40(3), 397–405.

Ibrir, S. and Diop, S. (1999). On continuous time differentiation observers. In *1999 European Control Conference (ECC)*, 2402–2406. IEEE.

Khalil, H.K. and Praly, L. (2014). High-gain observers in nonlinear feedback control. *International Journal of Robust and Nonlinear Control*, 24(6), 993–1015.

Khalil, H.K. and Priess, S. (2016). Analysis of the use of low-pass filters with high-gain observers. *IFAC-PapersOnLine*, 49(18), 488–492.

Mousavi, S. and Guay, M. (2021). A low-power multi high-gain observer design for state estimation in nonlinear systems. In *2021 60th IEEE Conference on Decision and Control (CDC)*, 5435–5440. IEEE.

Shakarami, M., Esfandiari, K., Suratgar, A.A., and Talebi, H.A. (2018). On the peaking attenuation and transient response improvement of high-gain observers. In *2018 IEEE Conference on Decision and Control (CDC)*, 577–582. IEEE.

Shakarami, M., Esfandiari, K., Suratgar, A.A., and Talebi, H.A. (2020). Peaking attenuation of high-gain observers using adaptive techniques: state estimation and feedback control. *IEEE Transactions on Automatic Control*, 65(10), 4215–4229.

Sussmann, H. and Kokotovic, P. (1991). The peaking phenomenon and the global stabilization of nonlinear systems. *IEEE Transactions on automatic control*, 36(4), 424–440.

Tréangle, C., Farza, M., and M'Saad, M. (2019). Filtered high gain observer for a class of uncertain nonlinear systems with sampled outputs. *Automatica*, 101, 197–206.

Vasiljevic, L.K. and Khalil, H.K. (2006). Differentiation with high-gain observers the presence of measurement noise. In *Proceedings of the 45th IEEE Conference on Decision and Control*, 4717–4722. IEEE.